

**INTERPRETATION OF HIGH RESOLUTION AEROMAGNETIC DATA TO ESTIMATE  
THE CURIE POINT DEPTH OF RAFIN REWA HOT SPRING, LERE LOCAL  
GOVERNMENT AREA OF KADUNA STATE.**

*Ezra D.,<sup>1</sup> Cyril G.A.<sup>2</sup> and Mba G.<sup>3</sup>*

<sup>1</sup>Department of General Studies, Nuhu Bamalli Polytechnic, Zaria, Nigeria.

<sup>2</sup>Department of Physics, Kaduna State University, Kaduna, Nigeria.

<sup>3</sup>Department of Mechanical Engineering, Nuhu Bamalli Polytechnic, Zaria, Nigeria.

*Abstract*

---

*This research was carried out to estimate the curie point depth in Rafin Rewa hot spring using high resolution aeromagnetic data interpretation. The study area is bounded by latitude 10.0°N to 10.5°N and longitude 8.5°E to 9.0°E. The study is necessitated by the need for alternative renewable energy sources for use in the country. Regional-residual separation was carried out on the total magnetic-intensity of the study area to yield the residual magnetic intensity after subtracting the regional field. Four blocks of the residual magnetic intensity data were extracted. The data of each block were zero padded and tapered to correct foredge effect. Then, they were subjected to Fourier transform. Spectral analysis was carried out on the Fourier transformed data and the results indicates that, the depth to top ranges from 1.25km to 1.9km with an average of 1.58km while the centroid varies from 4.2km to 4.9km with an average of 4.55km. It then, suggested that the study area undelain by a curie point depth between 6.8km to 8.4km withan average of 7.6km. The shallow Curie Point Depth recorded around Rafin Rewa hot spring is a reflection of high curie temperature which can be attributed to crustal thinning. The Curie Point Depth around the study area shows that the study area is a good source of geothermal energy. The Curie Point Depth around the northeast edge of the study area suggest a promising geothermal potential.*

---

*Keywords: Geothermal energy, Aeromagneticdata, Hot spring and Curie point depth*

**Introduction**

The growth of any country economically to eradicate poverty and insecurity depends on constant supply of energy from the sources that are cheap, accessible and non-toxic to the environment. If energy is not accessible it can contributes to the rise in poverty, deprivation and can cause depreciation on the economy of a country [1]. Energy and poverty reduction cannot be separated just as education and health. This is due to the fact that electric power supply is required by most machines and other electrical appliances used in industries offices and at homes.

Power generation is a major challenge to many countries including Nigeria [2]. The major source of generating power in Nigeria is hydroelectricity. The power generated through hydroelectricity is not enough throughout the year, since it depend on the volume of water available in the dam that drives the turbines which generates the electricity [2]. Meanwhile, the availability of water is based on two climatic seasons namely; rainy and dry seasons. There is normally inadequate water in the dam during dry season. Therefore, there is usually relative low electricity generated through hydro (www.usgs> special-topic-science). This condition could lead to incessant power outage or power rationing and this in turns can affect the economic development of the nation.

---

Corresponding Author: Ezra D., Email: ezradauda2014@gmail.com, Tel: +2348050575522

*Journal of the Nigerian Association of Mathematical Physics Volume 62, (Oct. – Dec., 2021 Issue), 51 –62*

More so, due to the combustion of fossil fuels that causes climate change [3], this has caused a serious universal concern. Over dependence on fossil fuel, their effects to the environment among other problems have caused a search for exploration of all available energy resources (especially renewable energy sources).

Geothermal (GT) energy is crucial in the long-term vision of providing secure abundant, renewable, cheap and reliable energy source for the nation. Geothermal energy is the form of heat energy that has its source in the Earth's subsurface as a result of decay of naturally occurring radioactive isotopes, such as Uranium-238, Thorium-235 and Potassium-40 [4]

Geothermal resources are converted into electricity by geothermal power plants [5]. This could be used to support the country's source of power generation and therefore could solve the problem of shortage of power in Nigeria. Similarly, the over-dependence on fossil fuel and its negative environmental effect could be minimized. Geothermal resources are available throughout beneath the Earth's subsurface, although they differ in concentration from one geological position to another [6]. To exploit geothermal resources, an initial identification of suitable areas is needed before its exploitation.

The Curie Point Depth is the depth at which the dominant magnetic mineral in the crust loses its ferromagnetic state and becomes paramagnetic due to rise in temperature [7]. This greatly relies on the geologic conditions of the area under consideration and is shallower in volcanic and geothermal fields [8]. The Curie point depth is assumed to be the depth where geothermal reservoirs are originated (Magnetic Chamber), where most geothermal reservoirs obtained their heat [9]. Assessment of differences of the Curie Isotherm of a place can give important information about the temperature distribution at depth and also the concentration of subsurface geothermal energy of the area [10]. It has been shown by measurement that a position with reasonable high temperature gradient and heat flow is of higher geothermal energy [10].

Spectral analysis method as the process of calculating and interpreting the spectrum of potential field data is chosen in this work for spectral depth is based on the principle that a magnetic field measured at the surface can be considered as an integral of magnetic signature from all depths [11].

The present work will serve as a detailed geophysical survey for better understanding of the geology of the study area in terms of sites for geothermal plants, and the knowledge when applied will boost the power sector which will then improve our nation's economy that is seriously affected by shortage of power supply.

**Study Area description**

The study area Rafin Rewa is situated in Lere Local Government of Kaduna State, Nigeria. Its geographical coordinates are 10°0'0" to 10°5'0" North and 8°0'5'0" to 9°0'0" East with an average elevation of 75m. It is located at the fringes of the Jos Plateau to the eastwest (Fig.1). An orogenic younger granite province of Jurassic age and directly east of the Rishiwa ring complex [12]. The area is well drained by a good network of rivers which takes their source from the neighboring ring complexes of the Jos (Fig 2).

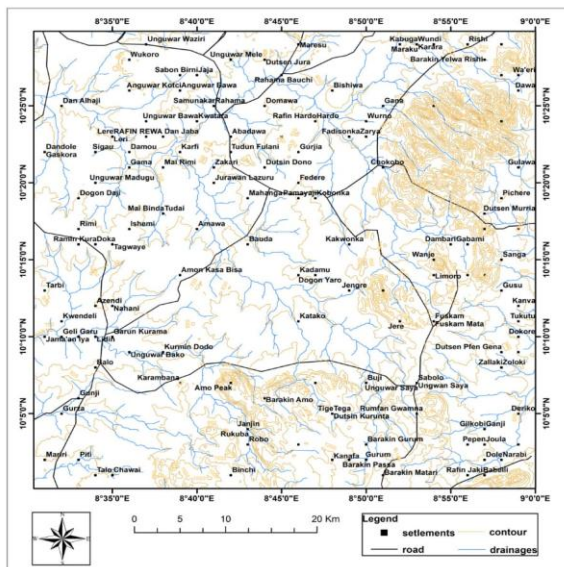


Figure 1: Geographical Map of the Study Area

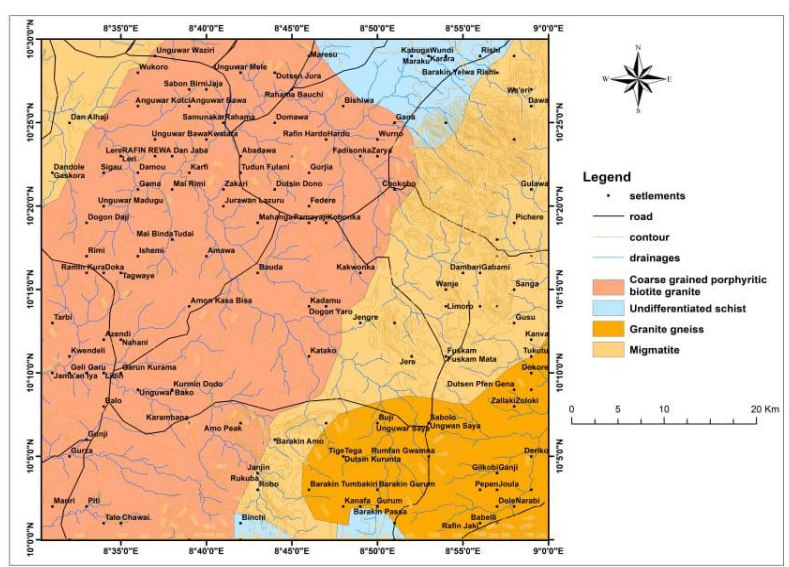


Fig 2: Geological Map of the Study Area

**Geology of the study area**

Rafin Rewa is a hot spring in Lere Local Government Area in Southern part of Kaduna State, Nigeria. The original name (with diacritics) is Lere. The town was established in 1870 by the fifth Sarkin Lere Muhammadu Dankaka, it is the headquarters of Lere Emirate and has an area of 320km<sup>2</sup> with a total population of 331,161 at the 2006 census. The town is located geographically at the latitude 10°39'0" North and 8°57'0" East with an average elevation of 75m above sea level.

The study area is a plain lowland area at the fringe of Jos Plateau which lies within the sub-humid ecological zone of Nigeria along guinea savannah vegetation belt with a rainfall of over 1600mm and wet season that last between May and October. The inhabitants are mostly farmers who grow mainly grains (Maize, millet, rice). In addition, these areas are well known to accommodate a good number of cattle herds. The study area shares boundaries with Kaura Local Government Area to the West and South, Kubau Local Government Area to the north west, Kano State to the north, Bauchi State to the east and Plateau State to southeast, respectively [13]. The topography of the area is more or less flat laying with migmatites occurring as low lying exposures, and prominent coarse grained porphyric biotite granite stand out conspicuously which is dotting the landscape. The geology of the Southeast constitutes dominant granite gneiss, the northeast through the southern region of Lere Local Government Area is dominated by migmatite which is the oldest rock pan Africa granite and bauchite. The bauchite is an unusual rock of acid to intermediate composition, containing in addition to Fayalite, which is extremely rich in iron pyroxenes (Ferroheden bergite and orthoferrosilite), [12]. While the region of northeast and part of south constitutes undifferentiated Schist. The hot spring (Rafin Rewa) is located around lere. An orogenic younger granite province of Jurassic age and directly east of the Rishiwa ring complex. protolith interspersed with felsic components. The biotite paragneiss often shown alternating band of dark and light- colored minerals. The coarse grained porphyritic biotite granite which are scattered over the area. The granite intrusive which belong to the older granite suite are the most widespread rocks in the area, and the most common varieties are biotite and coarse grained porphyritic granites with associated micaceous pegmatites [14].

**Materials for the study**

The following materials were used for this study, these include; Aeromagnetic Data (Sheet number 147), Oasis Montaj (software), Grapher (software), Suffer (software), Computer set, Printer and GPS.

The survey of the high-resolution aeromagnetic map (HRAM) data was conducted by Fugro Airborne Survey (Fugro) from 2003 to 2010. Part of this survey is sponsored by the World Bank through Nigeria's Sustainable Mineral Resources Management Project. Most of the surveys were carried out with a row spacing of 500 m and an average topographic gap of 80 m, resulting in a total of about 2 million row-km of data. Three Scintrex cesium vapor magnetometers installed on approximately seven Cessna Caravan fixed-wing aircraft at a time were used to acquire the data. The data logging interval is 0.1 seconds or less than 7 minutes. The projection methods used to process the data are Universal Transverse Mercator (UTM) and WGS 84 as a reference. The ellipsoid model used is Clarke 1880 (modified), 33°E central meridian, zoom factor of 0.9996, 500,000 m X deviation, 0 m Y deviation, and 50 m grid size are drawing specifications. Most of the data were collected between 2005 and 2009; therefore, the International Geomagnetic Reference Field (IGRF) 2005 model was used for magnetic declination and inclination calculations. Sheet 147, Lere, (Figure 3.) of HRAM data of 55×55 km was used. The data range is 8.5 °E to 9.0 °E in longitude and 10.0 °N to 10.5 °N in latitude.

The arrangement and storage of the data collected by Fugro are briefly stated: Column X represents longitude/easting, column Y represents latitude/northing, and column Z represents total magnetic intensity. For ease of handling, the total magnetic field strength, value (Z) of 33,000 nT has been removed. Therefore, after acquiring data from NGSA to derive Z Total, a simple arithmetic addition of 33,000 nT was performed on each value in column Z, and then it was considered to be the total magnetic intensity (in nT). The X and Y columns were georeferenced in the Universal Transverse Mercator (UTM) projection system and then set as the preferred columns. Finally, the data are gridded to generate a total magnetic intensity (TMI) grid map, as shown in Figure 3.

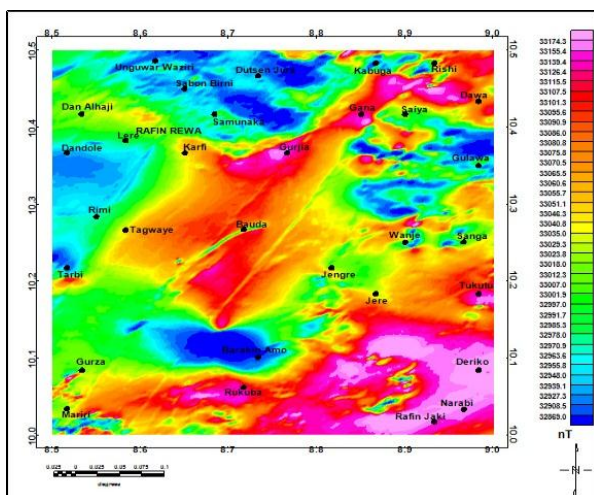


Figure 3: The total magnetic intensity map for the study area.

**Methods**

The grid of the aeromagnetic data was subjected to various data processing techniques before the Centroid method of Curie depth estimation was applied; regional-residual separation, and block division. The residual magnetic data was windowed to extract four blocks with a dimension of 27.5 × 27.5 km (see Figure 6). Each block was then subjected to zero-padding, tapering, and fast-Fourier transform.

**Regional-Residual Separation**

The earth’s magnetic anomaly field is a combination of the effects of both deeper, broader sources known as regional and local sources which are considered as noise and as well as anomalies of interest otherwise residual anomalies [15]. Several graphical and numerical techniques have been developed over the years to remove a particular anomaly type, of specified characteristics, within a field of superimposed anomalies of varying properties [15]. The least-square approach was adopted in this work. Removal of any field or noise from the potential field is a filtering process, ideal residual determination method will ‘pass’ without distortion only anomalies that are significant to the particular problem and will attenuate others. The basic idea is that anomalies that are to be removed should be completely removed and those to be kept should remain undistorted.

The ability to extrapolate beyond the data sequence, interpolate between data points, infer the presence of trends, or estimate characteristics that may be of interest to the geoscientists are tendencies of interest for the least-squares method as a filtering procedure [16]. In this regional-residual criterion, residual is the square of the deviation of the regional field from the observed (measured, TMI).

The regional uses a polynomial surface to reveal the residual features as the deviation from the observed field. The regional-residual separation of data into two components may be explained thus:

- a. It is based on geographic coordinates; this means that an observation (the total magnetic field data) is considered to be in part a function of the location of the observation.
- b. The surface is a linear function; it has the form  $Y = b_0 + b_1X_1 + b_2X_2\dots$ , where the b’s are coefficients and the X’s are some combination of the geographic coordinates.
- c. The specific linear functions chosen for the trend must minimize the squared deviation from the trend.

Hence, a linear function is an equation of the type

$$Y = b_0 + b_1X_1 + b_2X_2 \dots\dots\dots(1)$$

where the b’s are coefficients and the X’s are some combination of the geographic coordinates.

Equation (1) thus yields the values ( $\hat{Y}$ ) which are the regional components of the observation, which may be regarded as a linear function of some constant value  $b_0$  related to the mean observations, plus an east-west ( $b_1$ ) component (in this case, the latitudes) and north-south ( $b_2$ ) components (that is, the longitudes).

Hence, we obtain three normal equations:

$$\begin{aligned} \sum Y &= nb_0 + b_1 \sum X_1 + b_2 \sum X_2 \\ \sum X_1 Y &= b_0 \sum X_1 + b_1 \sum X_1^2 + b_2 \sum X_1 X_2 \\ \sum X_2 Y &= b_0 \sum X_2 + b_1 \sum X_1 X_2 + b_2 \sum X_2^2 \end{aligned} \dots\dots\dots(2)$$

In matrix form, equation 2 becomes:

$$\begin{bmatrix} n & \sum X_1 & \sum X_2 \\ \sum X_1 & \sum X_1^2 & \sum X_1 X_2 \\ \sum X_2 & \sum X_1 X_2 & \sum X_2^2 \end{bmatrix} \times \begin{bmatrix} b_0 \\ b_1 \\ b_2 \end{bmatrix} = \begin{bmatrix} \sum Y \\ \sum X_1 Y \\ \sum X_2 Y \end{bmatrix} \dots\dots\dots(3)$$

The TREND option in FILTER within GRID menu of Oasis montaj software was called to execute regional-residual separation. The solution to equation (3) for the aeromagnetic data was obtained solving the series of the equation that evolved from the substitution of the sums, sums of powers, and sums of cross-products required in equation (2). The coefficients  $b_0$ ,  $b_1$ , and  $b_2$  were found by solving the resulting set of simultaneous normal equations and the coefficients of the plane surface determined are then substituted into equation (3) and evaluated to obtain the regional surface ( $\hat{Y}$ ). The difference between the observed field data ( $Y$ ) and the regional field data ( $\hat{Y}$ ) gives the residual field data. Figures 2 and 3 shows the regional trending in the NE-SW direction, and residual magnetic field respectively for the study area.

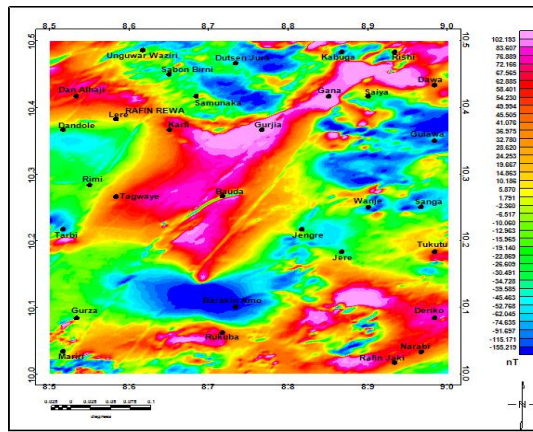
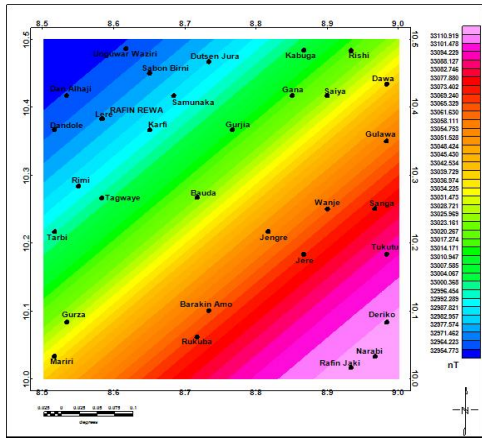


Figure 4: The regional magnetic field of the study area.

Figure 5: The residual magnetic field map for the study area.

**Block division**

The spectrum of the map only contains depth information to a depth of length  $(L)/2\pi$  [17]. If the source bodies have bases deeper than  $L/2\pi$ , the spectral peak occurs at frequency lower than the fundamental frequency for the map and cannot be resolved by spectral analysis [18]. On this basis, a large data size is usually adopted for spectral analysis. For example, in the estimation of depths to the Curie temperature in Oregon [19] divided a magnetic survey into overlapping cells ( $77 \times 77$  km) and calculated for each cell a radially average power spectrum.

In the evaluation of Curie depths of the entire Sokoto basin, Nigeria, [20] used a block size dimension of 110 km  $\times$  110 km. They based their choice after of [21] which suggests that the utilization of a small window width may be a fundamental error in the application of spectral methods for aeromagnetic interpretation. [22] used a block dimension of 89 km  $\times$  89 km in the determination of Curie point depth variations at the zone of continental collision in South-East Cameroon. A block size above 100 km  $\times$  100 km were used in the determination of the depth to the basement by [23] [24] used a varying block size in testing the use of aeromagnetic data for the determination of the Curie depth in California. The subregion dimension started from 90 km to 250 km, with an increment of 10 km. [25] used a block size of 128 km  $\times$  128 km in determining the Curie point depth map of Turkey. [26] used the block size of 300 km  $\times$  300 km in the determination of the Curie surface beneath Tarim Basin, China.

On the contrary [18] were constrained by the dimension of their data (40 km  $\times$  50 km) not to divide the magnetic data into overlapping grids, while [27] used a block size of 27.5 km  $\times$  27.5 km in the spectral analysis of a segment of Bida Basin, Nigeria.

The entire data size of the study area is 55bn/ km  $\times$  55 km thereby constraining the study to be limited to four blocks with a dimension of 27.5 km  $\times$  27.5 km. The warm spring is within block 4 as shown in Figure 6 below.

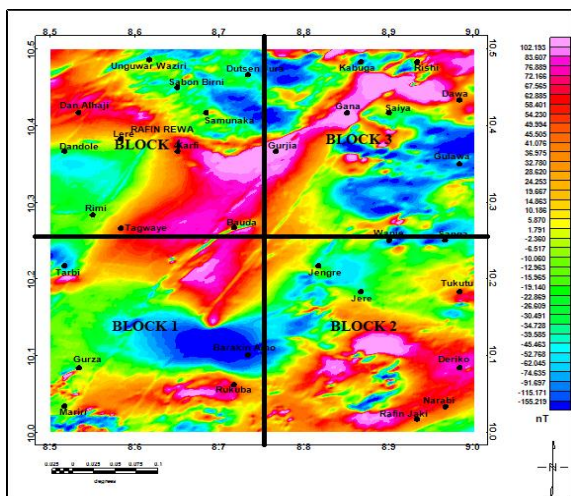


Figure 6: Map showing the division of the residual magnetic data into blocks.

### Edge effect correction

Mathematically, performing a Fourier transform on potential field data requires infinite long Time Series [28] and such will cause the Fourier-transform to develop non-zero values predominantly at lower frequencies (commonly called spectral leakage, meaning some frequencies tend to leak to other frequencies) [29]. It is standard practice, therefore, to multiply the data windows by a taper before performing a Fourier transform. The taper consists of a function smoothly decaying to zero near the ends of each window which is aimed at minimizing the effect of the discontinuity between the beginning and end of the time series [30].

Before a taper is introduced, it is necessary to zero-pad the magnetic data to retain the magnetic anomalies after tapering. Zero Padding simply consists of extrapolating the anomalies with zeroes [31]. The aliasing error that occurs in non-linear functions are often eliminated through zero-padding [32] [33].

Visible artifacts, due to fold-variation, that are related to the imprint of the block size can be avoided through tapering [34]. The cosine window, a taper apart from Hanning and others represents an attempt to smoothly set the data to zero at the boundaries while not significantly reducing the level of the windowed transform. This tapering will reduce the leakage of spectral power from a spectral peak to frequencies far away and also coarsens the spectral resolution by a factor  $\frac{1}{(1-a)}$  for the cosine tapers. Hence, if the real spectrum contains a strong low-frequency component, cutting the time series into short time windows without tapering may strongly distort the observed spectrum.

The grid of each block was transformed into the frequency domain by performing a Fast Fourier Transform (FFT) on it. The data processing, Regional-Residual separation, Zero Padding, Tapering, and FFT were performed using the Step-by-step filtering option in the MAGMAP menu of Oasis Montaj. The radial average power spectrum was then computed for the grid of each block using the Radial Average tool, Spectrum Calculation and Display option in the MAGMAP menu of Oasis Montaj. The computed result was extracted using an Excel package (Data – Get Data – From text). The worksheet contains several columns, most importantly, is column A, housing the angular frequency in cyc/km, and column C, housing the natural logarithm of the spectral power of the aeromagnetic data. Further computation was carried out using Grapher software.

### Curie Point Depth

The Curie point depth estimate of each block is achieved through the Spectra analysis of the magnetic data of the study area. Different approaches exist for estimation of depth to the bottom of magnetic sources, these include the spectral peak method [35] [17], centroid method [36] [37] [38] scaling spectral or power-law correction method [39], forward modeling of the spectral peak method [40] and modified-centroid fractal method [41] [20]. Nonetheless, the centroid method is one of the most commonly used approaches because it gives better estimates with fewer depth errors compared with others [21]. The Centroid method is the method applied in this work. The mathematical models of the centroid method are based on the examination of the shape of isolated magnetic anomalies introduced by [42] [43] and the study of the statistical properties of magnetic ensembles by [35]. Following the introduction of power spectral density of total magnetic field by [44], [38] showed that the top bound and the centroid of magnetic sources can be calculated from the power spectrum of magnetic anomalies, and consequently used to estimate the basal depth of the magnetic source. In practice, the centroid depth is calculated from the low wavenumber part of the wave number-scaled power spectrum as:

$$\ln(P(k)^{\frac{1}{2}}/k) = A - |k|Z_0 \dots \dots \dots (4)$$

where P(k) is the azimuthally averaged power spectrum, K is the Wavenumber  $\frac{2\pi}{k}$ , A is a constant and Zo is the centroid depth. The depth to the top of the magnetic source is similarly derived from the slope of the medium – to high-wavenumber portion of the power spectrum as:

$$\ln(P(k)^{\frac{1}{2}}) = B - |k|Z_t \dots \dots \dots (5)$$

where B is a constant and Zt is the depth to the top.

[38] advocated fitting the slope to a higher wavenumber part of the spectrum arguing that the linearized equation for the depth to the top is valid for wavelengths greater than the thickness of the layer. Fitting the slope to a higher wavenumber part of the spectrum as suggested by [38] leads to deeper magnetic bottom estimates that, at times, appear to be desirable [21]. Finally, the depth to the bottom of the magnetic source ( $Z_b$ ) is subsequently obtained from the relation [37]:

$$Z_b = 2Z_0 - Z_t \dots \dots \dots (6)$$

### Result and Discussion

The [35] method for estimating the depth extent of magnetic sources examines the patterns of anomalies. The method provides the relationship between the spectrum of the magnetic anomalies and the depth to magnetic sources by transforming the spatial data into frequency domain. To obtain the Curie point depth, spectral analysis of two-dimensional Fourier transform of the aeromagnetic data was made.

The spectral analysis on each of the blocks of aeromagnetic data were processed using the magmap extension option in

Oasis Montaj™, which enables two-dimensional frequency domain processing of potential field data. The results of the analysis are plotted on a logarithmic scale against the radial wave number. On such a plot, if a group of sources has a same depth, they will fall onto a line of constant slope (tangent of the line fitted to the power spectra). Thus, if there are sources at different depths, such as a shallow plutonic formation over a deep basement, the plot will be separated into two or more sections with different slope. The inverse of the angle of the slope is a measure of the depth of the source. This process was carried out to obtain the depth to the shallow ( $Z_t$ ) and deep ( $Z_0$ ) sources for the four sub-block.

**Results**

**Spectral Analysis**

Computing the Curie point depth of the study area is achieved by estimating the depths to the top, and the centroid of the magnetic source of each block. The depths to the top and the centroid was estimated from the plots of the power spectrum and wavenumber for block 1 (Figures 7 a - b). The depth to the top for block 1 is 1.3 km while the depth to centroid is 4.9 km.

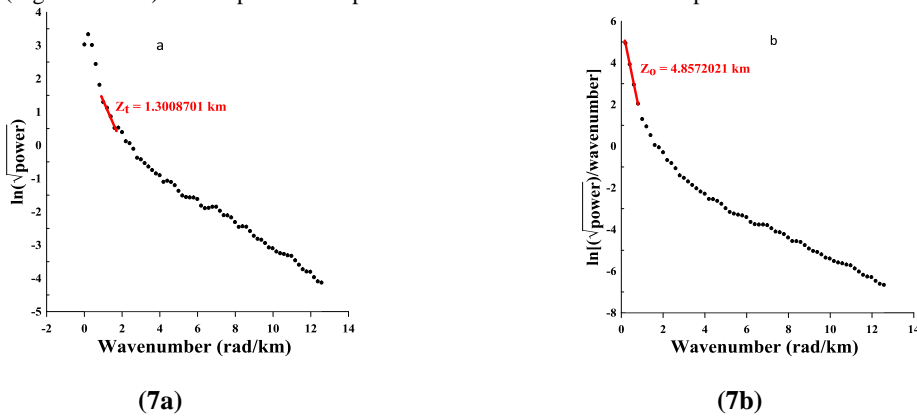


**Figure 7 (a & b): Spectral plot for block 1**

The depths to the top and the centroid was estimated from the plots of the power spectrum and wavenumber for block 2 (Figures 8 a - b). The depth to the top for block 2 is 1.3 km while the depth to centroid is 4.3 km.

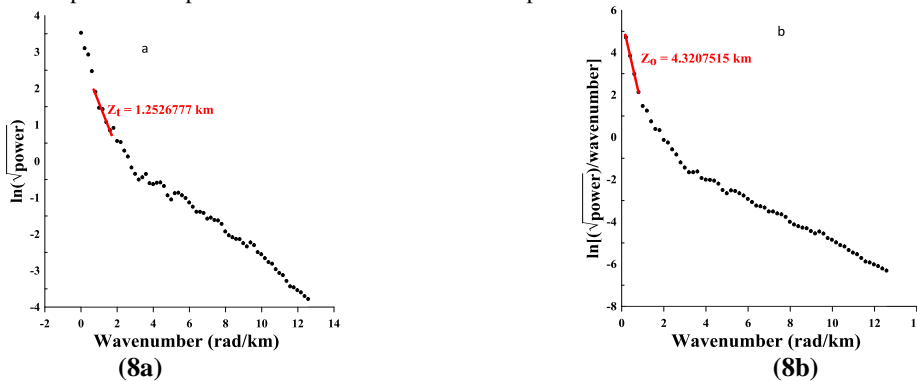


**Figure 8 (a&b): Spectral plot for block 2**

The depths to the top and the centroid was estimated from the plots of the power spectrum and wavenumber for block 3 (Figures 9 a - b). The depth to the top for block 3 is 1.6 km while the depth to centroid is 4.2 km.

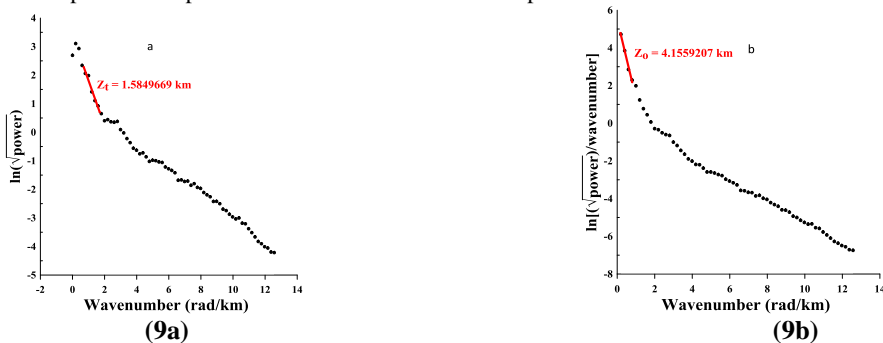


**Figure 9 (a&b): Spectral plot for block 3**

The depths to the top and the centroid was also estimated from the plots of the power spectrum and wavenumber for block 4 (Figures 10 a - b). The depth to the top for block 4 is 1.9 km while the depth to centroid is 4.8 km.

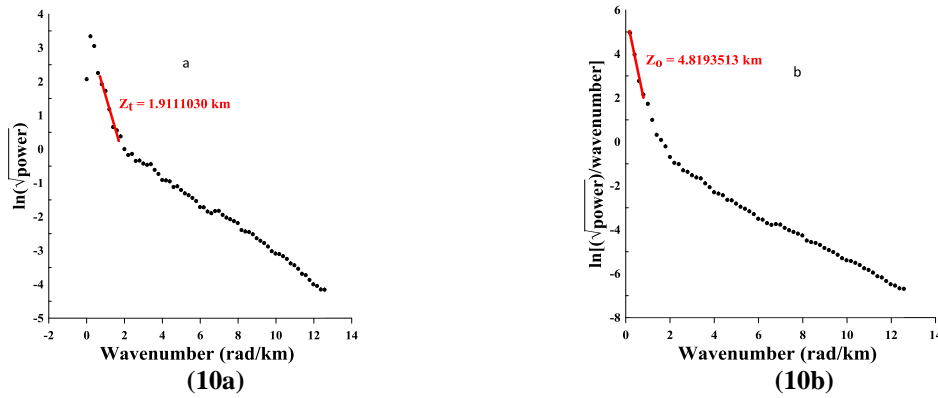


Figure 10 (a&b): Spectral plot for block 4  
 Map of depth to top

The depths to the top results for the blocks were used to draw the map of the depth to the top of the entire area to show its variation in the study area (Figure 11), it ranges from 1.25 km to 1.90 km. The depth to the top is shallow around Rukuba-Barakin Amo-Deriko-Narabi-Rafin Jaki of about 1.2 km while Sanga-Wanje-Jengre are about 1.4 km deep. Dan Alhaji-Lere-Dutsen Jura including Rafin rewa have deep depth to the top of about 1.85 km.

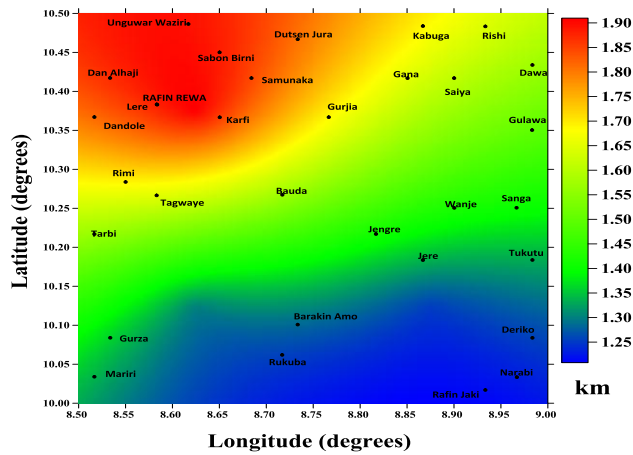


Figure 11: Map of the depth to the top for the study area  
 Map of Depth to the Centroid

The depths to the centroid results for the blocks were also used to draw the map of the depth to the centroid of the entire area to show its variation in the study area (Figure 12). The depth ranges from 4.15 km to 4.90 km. The eastern margin of the map from Rishi to Tukutu have shallow depth to the centroid of about 4.15 km, the central margin from Gurjia to Rafin Jura have depth to the centroid of about 4.45 km, and western margin from Dan Alhaji to Mariri including Rafin rewa have depth to the centroid of about 4.9 km.

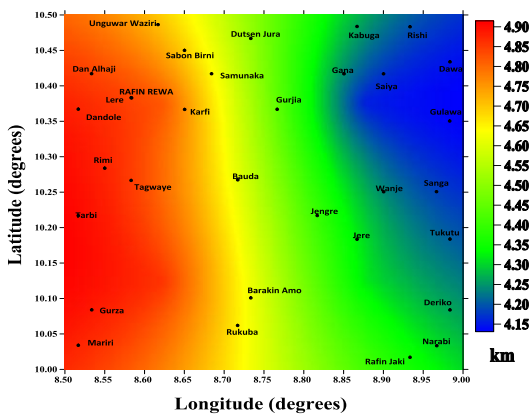
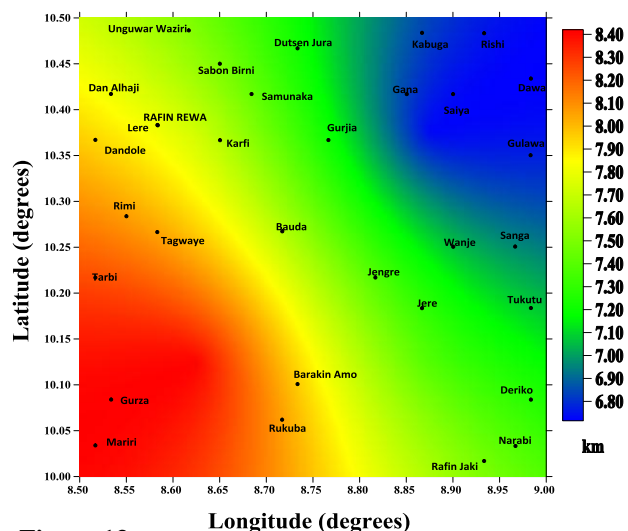


Figure 12: Map of the depth to the centroid of the study area.



**Map of Curie point depth**

The result of the depths to the top and the centroid were used to compute the depth to the Curie point depth of the study area (equation 6) to show the variation Curie depths of the area (Figure 13). The CPD of the study area ranges from 6.80 km to 8.40 km.



**Figure 13:**  
**Map of the depth to the Curie point of the study area**

The study area is characterized by increase in the CPD in the southwest direction around Mariri to Tarbi with CPD of about 8.4km. It is believed to be influenced by the depths to the centroid (fig 12) While the northeast edge of the study area around Rishi to Gulawa has the shallowest CPD of 6.8km, Rafin Rewa region is characterized by a CPD of about 7.8km which is shallower than the 10km for geothermal energy attributable to volcanic activity. As shallow CPD is a reflection of a high curie temperature which could be an indication of crustal thinning.

**Discussion**

Curie temperature may provide a proxy for temperature-at-depth in places where heat-flow information is inadequate [24]. Curie point depth varies greatly with geologic settings [38] [45]. it was reported to be shallower than 10 km for geothermal energy attributable to volcanic activity, which are commonly associated with plate boundaries and other geodynamic environments. However, Curie point depths ranging between 15 km and 25 km are as a result of island arcs and ridges, and deeper than 20 km in plateaus and trenches [20].

The study area is characterized by increase in the Curie point depth in the southwest direction (Figure 4.7), it is believed to be influenced by the depths to the centroid (Figure 4.6). The southwest edge of the study area (Gurza, Mariri, and Tarbi) has the deepest CPD of 8.40 km while the northeast (Kabuga, Rishi, Gana, Saiya, Dawa, and Gulawa) has the shallowest CPD of 6.80 km, Rafin Rewa region is characterized by a CPD of about 7.8 km which is shallower than the 10 km for geothermal energy attributable to volcanic activity. A shallow Curie point depth is a reflection of a high Curie temperature which could be an indication of crustal thinning [25].

**Conclusion and Recommendation**

This project was carried out to determine the geothermal energy source in Rafin Rewa through the interpretation of the aeromagnetic data of Lere. The centroid method was employed to determine the Curie point depth, geothermal gradient, and heat-flow of the study area. The Rafin Rewa characterized by a CPD of about 7.8 km, geothermal gradient of 0.08 °C/m, and heat-flow of 0.19mW/m<sup>2</sup>. The shallow CPD recorded around Rafin Rewa is a reflection of high Curie temperature which can be attributed to crustal thinning. The CPD around Rafin Rewa is shallower than the geothermal energy attributable to volcanic activity. The CPD around the northeast edge of the study area suggest a promising geothermal potential.

Base on the findings of research, it is recommended that the: A structural investigation be carried out in the study area to delineate a possible conduit of the fluid gushing out of the spring and a magnetotelluric survey be conducted at the identified promising site to ascertain the geothermal situation of the area at depth.

## REFERENCES

- [1] Asad A., Yaping L., Jie Y., Abbas A.C., Samma F.R. Ji I., and Shah Z. (2020). "How does energy Poverty affects economic development?" *panel data analysis of South Asia countries. Environmental Science and pollution Research*, 27,31623-31635.
- [2] Ikuobase Emovon, Olusegun D. Samuel, Chinedum Ogonna Mgbemena (2018). Electric power generation crisis in Nigeria: A review of causes and solutions. *International journal of integrated engineering*. 10(1): doi:10.30880/ijie.2018.10.01.008.
- [3] Frederica Perera (2018). Effect of Combusion of fossil fuel. *International journal of Environmental Research and Public Health. IJERPH* 15 (1)
- [4] Sanders, Robert (2002). *Radioactive potassium may be major heart source in Earth core UcBertheley News* Retrieved 2007-02-28.
- [5] Abdullahi B.U., Rai J.K., Oloitan O.M & Musa Y.A (2014). A Review of the correlation between Geologand Geothermal Energy in North-Eastern Nigeria. *IOSR Journal of Applied Geology and Geophysics*. Vol.2(3) 74-83.
- [6] Garba M.L, Kurowska E., Schoeneich K., Abdullahi I. (2012). Rafin Rewa Warm Spring, A New Geothermal Discovery, *American International Journal of Contemporary Research*, 2, ( 9) 1-8.
- [7] Abraham E.M, Nkitnan E.E (2017). Review of Geothermal Energy Research in Nigeria: *The Geoscience front international Journal of Earth Science Geophysics* 3;015.
- [8] Aliyu A., Salaka K.A., Adewumi T.,& Mohammed A (2018).). Interpretation of High Resolution Aeromagnetic Data to Estimate the Curie Point Depth Isotherm of part of Middle Benue Trough, North-East, Nigeria. *Physical Science International Journal* 17(3) 1-9.
- [9] Etetta B.E & Udensi E.E (2012). Investigation of the Curie Depth Isotherm from the magnetic fields of Eastern Sector of Central Nigeria. *Journal of Geological Sciences*. 2(4) 101-106.
- [10] Tselentis G.A (1991) An attempt to define curie depth in Greece from Aeromagnetic and heat flow data. *PAGEOPH*. 136(1) 87-101.
- [11] Ajama o; Udensi E.E; Momoh M; Rai J.K and Muhammad S.B (2014). Spectral Depths Estimation of Subsurface Structures in part of Borno Basin, North eastern Nigeria, using Aeromagnetic Data. *Journal of Applied Geology and Geophysics*. 2 (2) 55-60. Tectonic implications.
- [12] Oyawoye M.O., and Makanjoula A.R.(1972). Ground water potential of the Edge-Mopa basement area, central Nigeria. *Journal of African Earth Science* 1(3) 339-342.
- [13] Abenga J.N., Enwezor F.N., Lawani F.A., Osue H.O & Ikemereh E.C (2004). *A description of the Lere Local Government Area*. Pathology, Epidemiology and Statistics Division, Nigeria Institute for Trynanosnmiasis Research. Kaduna, Nigeria. *Revue.Elev. Vet. Pays.trop-200*, 57 (1-2) : 45-48.
- [14] Britten, R. (2017). *Regional Metallogeny and genesis of a new deposit type. Disseminated Awaruite(Ni3Fe) mineralization hosted in the cache creek Terrane*, *Economic Geology*. 112(3): 517-550.
- [15] Hinze, W.J. (1990). *The role of Gravity and Magnetic Methods in Engineering and Environmental Studies*, In; Ward, S.H. Ed., *Geotechnical and Environmental Geophysics*, Society of Exploration Geophysics, 1; 75 – 126.
- [16] Davis, J.C. (1973). *Statistics and Data Analysis in Geology*. John Wiley and Sons Incorporation, New York, 44 – 120.
- [17] Shuey R.T, Schellinger D.K, Tripp A.C., and Alley, L.B. (1977) Curie depth determination from aeromagnetic spectra, *Geophysical Journal of the Royal Astronomical Society*, 50: 75-101.
- [18] Salem A, Ushijima K, Elsirafat A, Mizunaga H (2000). *Spectral analysis of aeromagnetic data for geothermal reconnaissance of Quseir area, northern Red Sea, Egypt*. Proceedings of the world geothermal congress:1669–1674
- [19] Connard G, Couch R, Gemperle M (1983). *Analysis of aeromagnetic measurements from the Cascade Range in the Central Oregon*. *Geophysics* 48:376–390
- [20] Nwankwo, L.I., and Shehu, A.T. (2015). Evaluation of the Curie-point depths, geothermal gradients and near-surface heat flow from high-resolution aeromagnetic (HRAM) data of the entire Sokoto Basin, Nigeria. *Journal of Volcanology and Geothermal Research*, doi: 10.1016/j.jvolgeores.2015.09.017.

- [21] Ravat D, Pignatelli A, Nicolosi I and Chiappini M (2007). A study of spectral methods of estimating the depth to the bottom of magnetic sources from near-surface magnetic anomaly data, *Geophysical Journal International*, 169: 421-434.
- [22] Feumoe, A.N.S. and Ndougsa-Mbarga, T. (2017). Curie Point Depth Variations Derived from Aeromagnetic Data and the Thermal Structure of the Crust at the Zone of Continental Collision (South-East Cameroon). *Geophysica*, 52(1); 31 – 45.
- [23] Teknik, V. and Ghods, A. (2017). Depth of magnetic basement in Iran based on fractal Spectral analysis of aeromagnetic data. *Geophysical Journal International*, 209; 1878 –1891. The NEED Project < [www.NEED.org](http://www.NEED.org)>.
- [24] Ross H.E, Blakely R.J and Zoback M.D(2006). Testing the use of aeromagnetic data for the determination of Curie depth in California. *Geophysics*, 71(5) L51–L59, doi:10.1190/1.2335572.
- [25] Aydin, I., Karat, H.I., and Koçak, A. (2004). Curie-point depth map of Turkey. *Geophysical Journal International*, 162. 633 – 640.
- [26] Gao, G., Kang, G., Li, G., and Bai, C. (2015). Crustal magnetic anomaly and Curie surface beneath Tarim Basin, China, and its adjacent area. *Canadian Journal of Earth Science*, 52; 1 – 11.
- [27] Tsepav M.T and Mallam A (2017). Spectral Depth Analysis of some Segments of the Bida Basin Nigeria, using Aeromagnetic Data. *Journal of Applied Science and Environmental Management*, 21(7); 1330 – 1335.
- [28] Gubbins, D. (2012). *Time Series Analysis and Inverse Theory for Geophysicists*. Cambridge University Press. <https://doi.org/10.1017/CBO9780511840302>
- [29] Xu, S., and Yu, Z., Pham, D, and Lambaré, G. (2005). Antileakage Fourier transform for seismic data regularization. *Geophysics*, 70(4):V87-V95. DOI: [10.1190/1.1993713](https://doi.org/10.1190/1.1993713).
- [30] Pilz, M. and Parolai, S. (2012). *Journal of Atmospheric Sciences*, 28, 1074, [https://doi.org/10.1175/1520-0469\(1971\)028<1074:OTEOAI>2.0.CO;2](https://doi.org/10.1175/1520-0469(1971)028<1074:OTEOAI>2.0.CO;2) Tapering of windowed time series. DOI: 10.2312/GFZ.NMSOP-2\_IS\_14.1
- [31] Constaldo, R., Fedi, M., and Florio, G. (2014). Multiscale estimation of excess mass from gravity data. *Geophysical Journal International*, 197; 1387 – 1398.
- [32] Orszag, S.A. (1971). *The Elimination of Aliasing in Finite-Difference Schemes by Filtering High-Wavenumber Components*.
- [33] Donnelly, D., and Rust, B. (2005). *The Fast Fourier Transform for Experimentalists. Part II. Convolutions, Computing in Science Engineering*, 7, 92–95, <https://doi.org/10.1109/MCSE.2005.82>, <https://ieeexplore.ieee.org/stamp/stamp.jsp?tp=&arnumber=1463142>, 2005.
- [34] Bekara, M. (2013). *Taper design for block processing of seismic data*. *Geophysics*, 78(3); A19 – A22.
- [35] Spector, A and Grant F.S.(1970). Statistical model for interpreting aeromagnetic data. *Geophysics*, 35(2); 293–302.
- [36] Bhattacharyya, B.K and Leu, L.K (1977). Spectral analysis of gravity and magnetic anomalies due to Rectangular prismatic bodies. *Geophysics* 42,41-50.
- [37] Okubo Y, Graf, R.J., Hansen R.O, Ogawa, K., and Tsu, H. (1985) Curie. *point depths of the island of Kyushu and surrounding area, Japan*; *Geophysics*, 50 (3) 481– 489, doi:10.1190/1.1441926.
- [38] Tanaka A., Okubo Y. & Matsubayashi O (1999). Curie point depth base on spectrum analysis of the magnetic anomaly data in East and Southeast Asia. *Tectonophysics*. 306 (1) 461-470.
- [39] Maus, S. & Dimri, V., 1996. Depth estimation from the scaling power spectrum of potential Fields? *Geophysical Journal International*, 124(1); 113–120.
- [40] Finn, C.A. and Ravat, D. (2004). Magnetic Depth Estimates and Their Potential for Constraining Crustal Composition and Heat Flow in Antarctica. *Eos Transactions. American Geophysical Union*, 85(47); T11A-1236.
- [41] Bansal A.R., Gabriel, G., Dimri, V.P., and Krawczyk, C.M. (2012). Estimation of depth to the bottom of magnetic sources using modified centroid method for fractal distribution of sources: An application to aeromagnetic data in Germany. *Geophysical Journal International*, 76(3); 11 – 22.
- [42] Bhattacharyya B. K and Leu L. K (1975) Analysis of magnetic anomalies over Yellowstone National Park: Mapping of Curie point isothermal surface for geothermal reconnaissance. *Journal of Geophysical Research*, 80 (32); 4461–4465, doi: 10.1029/JB080i032p04461.
- [43] Bhattacharyya B. K and Leu L. K (1977) *Spectral Analysis of gravity and magnetic anomalies due to rectangular prismatic bodies*. *Geophysics*, 42; 41–50 doi:10.1190/1.1440712.

- [44] Blakely R. J (1995). *Potential theory in gravity and magnetic applications*: Cambridge University Press.
- [45] Salk, M., Pamukcu, O., and Kaftan, I. (2005). Determination of Curie point depth and heat flow from magsat data of western Anotolia. *Journal of Balkan geophysical society*, 8(4),149 – 160.  
[www.usgs.gov/special-topic/science](http://www.usgs.gov/special-topic/science).